

Robust quantification of cellular mechanics using optical tweezers

Wessel S. Rodenburg,^{1,2} Sven F. A. Ebben,¹ and Jorine M. Eeftens^{1,2,*}

¹Institute for Molecules and Materials, Radboud University, Nijmegen, the Netherlands and ²Radboud Institute for Molecular Life Sciences, Radboud University, Nijmegen, the Netherlands

ABSTRACT The mechanical properties of cells are closely related to function and play a crucial role in many cellular processes, including migration, differentiation, and cell fate determination. Numerous methods have been developed to assess cell mechanics under various conditions, but they often lack accuracy on biologically relevant piconewton-range forces or have limited control over the applied force. Here, we present a straightforward approach for using optically trapped polystyrene beads to accurately apply piconewton-range forces to adherent and suspended cells. We precisely apply a constant force to cells by means of a force-feedback system, allowing for quantification of deformation, cell stiffness, and creep response from a single measurement. Using drug-induced perturbations of the cytoskeleton, we show that this approach is sensitive to detecting changes in cellular mechanical properties. Collectively, we provide a framework for using optical tweezers to apply highly accurate forces to adherent and suspended cells and describe straightforward metrics to quantify cellular mechanical properties.

WHY IT MATTERS Cell mechanics are closely related to biological function, and altered mechanical properties of cells have been implicated in disease. The mechanical properties of cells can be studied by quantifying how cells deform over time in response to externally applied forces. Optical tweezers allow for mechanical manipulations with nanometer precision and force application at single-pN resolution. Although widely used in single-molecule and microrheology experiments, the use of optical tweezers to study whole-cell mechanics has been limited. Here, we describe a method to deform adherent and suspended cells using optical tweezers under the control of a force-feedback system. This approach allows us to extract several mechanical properties of cells from a single measurement while maintaining precise control over the applied force.

INTRODUCTION

Cells are continuously exposed to mechanical forces *in vivo*. These forces can be generated internally, such as through actomyosin contractions, or can originate from the local environment. For instance, blood and immune cells experience shear stresses in the circulation, migrating cells encounter forces from interactions with the extracellular matrix, and cells within tissues are continuously exposed to compressive stress. The physical and mechanical properties of cells are crucial to sense, resist, and respond to such forces and are, therefore, precisely tuned to align with their function and the local environment (1–5). The intricate

interplay between cell mechanics, mechanosensing, and biological response is vital to many cellular processes, including adhesion, migration, differentiation, and cell fate determination (6–11). Importantly, alterations in cell mechanics have been associated with aging (12,13) and disease (14–16).

The crucial role of cellular mechanics in health and disease has motivated the development of methodologies that apply external forces to cells to quantify their mechanical properties, each with advantages and limitations (recently reviewed in (17)). The most routinely used technique is atomic force microscopy (AFM), in which the tip of a cantilever is used to indent cells. AFM can apply relatively high forces in the nanonewton (nN) regime, resulting in large cellular deformations. Although sub-pN stability is reached with AFM in single-molecule force spectroscopy (18), cantilevers used for the quantification of cell mechanics generally lack this accuracy (19,20). Another commonly applied

Submitted November 26, 2024, and accepted for publication February 6, 2025.

*Correspondence: jorine.eeftens@ru.nl

Editor: Jorg Enderlein.

<https://doi.org/10.1016/j.bpr.2025.100199>

© 2025 The Author(s). Published by Elsevier Inc. on behalf of Biophysical Society.

This is an open access article under the CC BY-NC-ND license (<http://creativecommons.org/licenses/by-nc-nd/4.0/>).



technique is micropipette aspiration, which deforms cells by applying a local suction pressure. Although relatively easy to implement, micropipette aspiration lacks spatial and temporal resolution, complicating accurate quantification of cellular deformation (21). Finally, recently developed flow-based techniques, which deform suspended cells through shear fluid forces, enable high-throughput measurements but have limited options for parallel confocal visualization and lack precise control over the applied stress (22,23). This results in heterogeneous force application across cells, making robust quantifications challenging.

Most of our current understanding of cell mechanics originates from studies on cells adhered to plastic or glass surfaces. A limitation of this approach is that the properties of the underlying surface can directly influence cell mechanics (2,4,5,8). Additionally, mechanical perturbations can have profoundly different effects depending on whether cells are adhered to a surface or not (24). Although technically more challenging, measuring cellular mechanics in the suspended state eliminates any influence from the surface. Therefore, a comprehensive mechanical characterization of cells should ideally include measurements performed on both adherent and suspended cells. Taken together, the ideal technique to study how cells respond to external forces would offer 1) high accuracy in force quantification; 2) precise control over the applied force and its duration, ensuring all cells undergo the same force; 3) a parallel visual readout (through bright-field and/or confocal microscopy); and 4) the ability to quantify the mechanical properties of cells in both the adherent and suspended states.

Optical tweezers operate by using a near-infrared focused laser to trap micron-sized beads. Moving these optically trapped beads allows for mechanical manipulations of various samples with nanometer precision. Forces can be quantified at single-pN resolution by tracking the deflection of the bead from the optical trap center, often through back-focal-plane interferometry. Although this technique has been widely employed in single-molecule studies (25), it also holds significant potential as a technique for measuring cellular mechanics (26,27). Previous work has extensively employed optical tweezers to mechanically characterize several cellular components, including the cell membrane (28,29), cytoplasm (30), and (isolated) nuclei (31,32), and to visualize how forces are transmitted within cells (33–35). However, the use of optical tweezers to quantify whole-cell mechanics, especially upon mechanical perturbation, has been limited and mostly restricted to red blood cells (36–41). To date, a general and detailed description of using optical tweezers to perform mechanical measurements on whole cells is lacking.

Here, we present a robust method to quantify the mechanical properties of adherent and suspended cells using optical tweezers under the control of a force-feedback system, allowing for the direct quantification of the deformability, stiffness, and creep response from a single measurement. We use optically trapped polystyrene beads to indent adherent and suspended cells along the lateral direction. We show that the use of a force-feedback system allows for accurate force application in the pN range with minimal deviations. To validate that our approach accurately quantifies the mechanical properties of cells, we manipulated the cytoskeleton through inhibition of myosin II activity and actin polymerization, showing that these mechanical perturbations significantly soften cells. Our findings demonstrate that optical tweezers are well suited for precise mechanical measurements on adherent and suspended cells. Finally, we provide an overview of straightforward metrics for the quantification of cellular mechanics.

MATERIALS AND METHODS

Cell culture

HEK293T cells were cultured in DMEM GlutaMax (Gibco, Waltham, Massachusetts) supplemented with 10% fetal bovine serum and 1% penicillin-streptomycin. Cells were grown at 37°C and 5% CO₂.

Preparation of cells for optical tweezers experiments

For optical tweezers experiments with adherent cells, μ -Slides (0.4 mm, Ibidi, Fitchburg, Wisconsin) were precoated with 10 μ g/mL fibronectin (Sigma-Aldrich, St. Louis, Missouri, 341631) for 2 h at room temperature (RT). Cells were seeded overnight to obtain a confluency of roughly 50%. The medium was then replaced by fresh medium supplemented with 25 mM HEPES (Gibco) containing 3 μ L of uncoated polystyrene beads (3.15 μ m, 5% w/v, diluted 1:200 in PBS, Spherotech, Lake Forest, Illinois). When combined with confocal imaging as in Fig. 1 C, cells were stained with CellMask Green Plasma Membrane Stain (1:1000, Thermo Fisher Scientific, Waltham, Massachusetts) for 10 min directly before starting optical tweezers experiments. Optical tweezers experiments with adherent cells were performed for a maximum of 2–3 h at RT.

For experiments with suspended cells, cells grown until roughly 80% confluency were trypsinized, pelleted down, and resuspended in fresh medium supplemented with 25 mM HEPES (Gibco). \sim 3000 suspended cells and 3 μ L of uncoated polystyrene beads (3.15 μ m, 5% w/v, diluted 1:200 in PBS, Spherotech) were added into uncoated μ -Slides (0.4 mm, Ibidi). Cells were incubated in the slide for \sim 15–30 min before starting optical tweezers measurements. Optical tweezers experiments with suspended cells were performed for a maximum of 1–2 h at RT.

Optical trapping and force application

A dual-trap optical tweezers setup (C-trap, LUMICKS, Waltham, Massachusetts) equipped with a nanostage was used. Slides were positioned between a water objective and an oil immersion condenser. Infrared laser beams (1064 nm) were used for the optical trapping of beads. A single bead (for measurements with

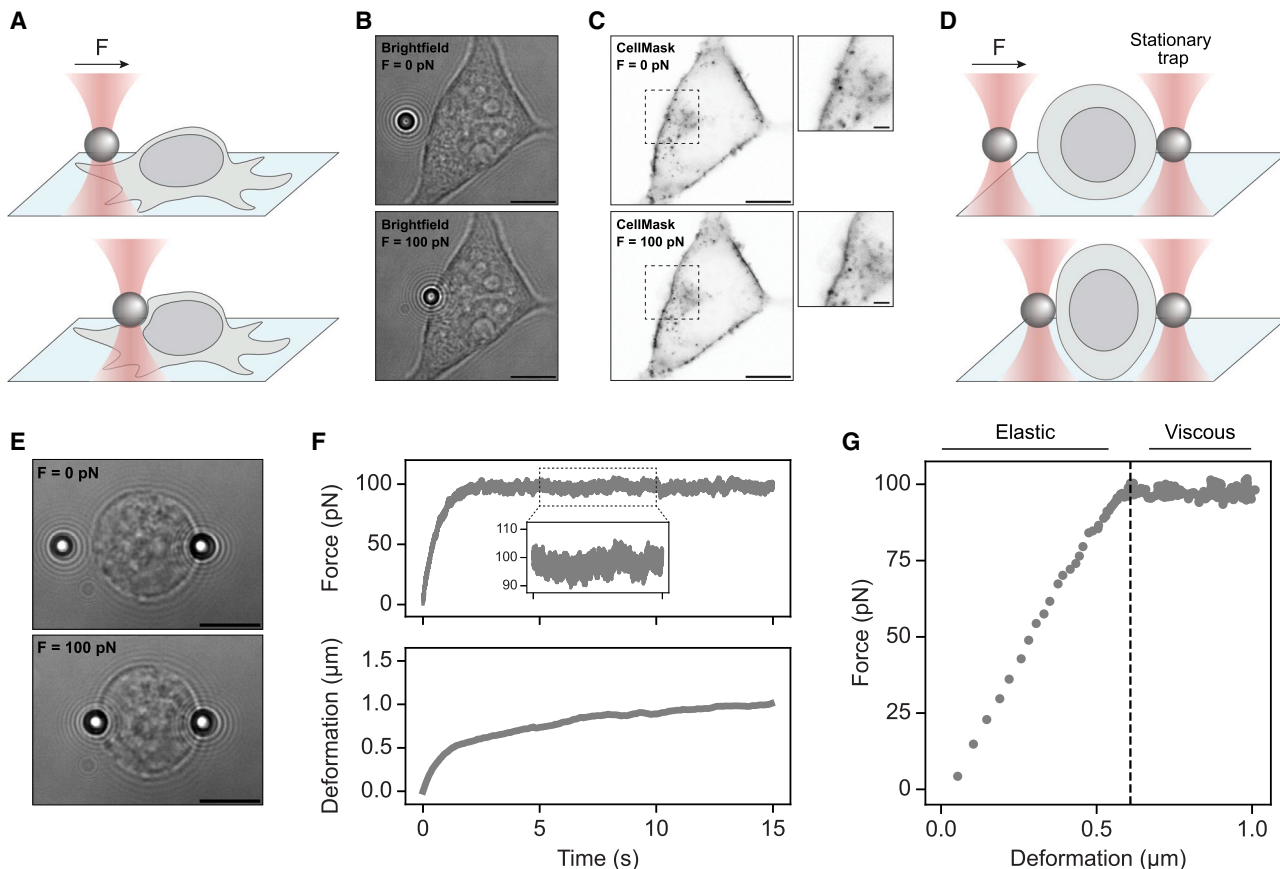


FIGURE 1 Deformation of adherent and suspended cells using optical tweezers. (A) Schematic illustration of an optical tweezers experiment on adherent cells. Cells are seeded on a fibronectin-coated surface. A single bead is optically trapped and moved along the lateral direction to apply force. (B) Bright-field images of an adherent cell before force application (*top*) and during 100 pN force application (*bottom*). Scale bars, 10 μm . (C) Inverted confocal images of the cell membrane (CellMask plasma membrane marker) corresponding with the bright-field images in (B). Scale bars, 10 μm . Zoomed-in insets show local deformation. Scale bars, 2 μm . (D) Schematic illustration of an optical tweezers experiment on suspended cells. A stationary optically trapped bead serves to immobilize the cell while the other is moved along the lateral direction to apply force. (E) Bright-field images of a suspended cell before force application (*top*) and during 100 pN force application (*bottom*). Scale bars, 10 μm . See also [Video S1](#). (F) Force (*top*) and corresponding deformation (*bottom*) plotted over time for the suspended cell shown in (E). A constant load of 100 pN was applied to the cell for ~ 10 s while the deformation was monitored. (G) Force-deformation curve of the suspended cell shown in (E). Dashed line indicates the moment the target force of 100 pN is reached.

adherent cells) or two beads (for measurements with suspended cells) were optically trapped and moved to the z-plane, where cells were visually in focus by moving the nanostage along the z-axis. For measurements with adherent cells, a single optically trapped bead is positioned at a few μm distance from the side of a cell (see also [Fig. 1 B, top image](#)). The optical trap is subsequently moved along the lateral (x) direction under the control of a force-feedback system to apply force to the cell. The force-feedback system quantifies deviations from a predefined target force at a rate of 31.3 Hz and adjusts the optical trap position accordingly with a maximum step size of 50 nm. For measurements with suspended cells, two optically trapped beads are positioned on opposite sides of a cell along the lateral (x) axis, both at a few μm distance of the cell. One bead is manually moved toward the cell along the lateral (x) axis until contact is made (see also [Fig. 1 E, top image](#)). Force is then applied to the cell by moving the other bead along the lateral (x) direction under the control of a force-feedback system, similar to the measurements with adherent cells. For both adherent and suspended cell measurements, a constant load (i.e., the target force) was applied to the cell for at least 10 s. Force data were acquired at a rate of 78,125 Hz using back-focal-plane detection. The

positions of the beads were acquired at a rate of 15 Hz using bead tracking software (LUMICKS).

Drug treatments

Latrunculin-A (Sigma, Burlington, Massachusetts, L5163) was diluted in DMSO and used at a final concentration of 1 μM . Blebbistatin (Sigma, B0560) was diluted in DMSO and used at a final concentration of 20 μM . Cells were incubated with the inhibitors (or an equivalent amount of DMSO as a control) for ~ 15 min before starting optical tweezer experiments.

Data analysis

Data analysis was performed using Pylake Python package (LUMICKS) and custom-made Python scripts. First, the starting point of deformation (i.e., the point of contact between the bead and the cell) was calculated for each measurement. We defined the point of contact as the bead position (for adherent cells) or the distance between the beads (for suspended cells) when the force first

reaches a value below 0 pN (starting from the maximum force) (see also Fig. S1, A and B). The deformation of the cell was calculated over time by comparing the position of the bead or the distance between the beads relative to the point of contact. Mechanical properties are extracted from the resulting force-deformation curves. The deformation was defined as the amount of deformation 10 s after reaching the target force. The spring constant was calculated as the slope of the linear part of the force-deformation curve through linear regression analysis. For suspended cells, we additionally quantified the cell diameter to derive the strain—that is, the ratio of deformation over the cell diameter. The cell diameter was quantified as the distance between the center of the two beads at the point of contact minus the bead diameter. The creep deformation was defined as the additional deformation measured 10 s after reaching the target force. The average creep response was fitted to Eq. 1:

$$\Delta x * \left(1 - e^{\left(-\frac{t}{\tau}\right)}\right), \quad (1)$$

from which best fit values of Δx (creep extent) and τ (relaxation time) were derived. In 7 out of 121 measurements, the cell exhibited negative creep (i.e., the bead being pushed back by the cell), and these measurements were excluded from the analysis of the creep response.

Statistical analysis

Datasets were tested for normality using Shapiro-Wilk test ($\alpha = 0.05$). Two-sample *t*-tests were used to compare normally distributed data. Non-normally distributed data were compared using the Mann-Whitney U test. In both cases, *p* values lower than 0.05 were considered statistically significant. Data are presented as mean \pm SE.

RESULTS

Cellular deformation through force application with optically trapped beads

Optical tweezers can capture and precisely maneuver beads trapped within a focused laser. Force is measured by tracking the displacement of the trapped bead from the center of the optical trap. In this study, we used optically trapped polystyrene beads (3.15 μm in diameter) to deform adherent and suspended cells. For measuring on adherent cells, a single bead is optically trapped, positioned at a few μm distance of the side of a cell, and then moved along the lateral direction to deform the cell (Fig. 1 A). To visualize the nature and extent of cellular deformation in response to piconewton (pN)-range forces, cells were imaged before and while applying force through a combination of bright-field and confocal microscopy (Fig. 1, B and C). Using CellMask, a fluorescent dye that labels the plasma membrane, we clearly observed local indentation of the cell (Fig. 1 C). In contrast to adherent cells, measuring on suspended cells requires two optically trapped beads. One optical trap remains stationary and serves to stabilize the position of the cell while the other trap moves along the lateral direction (Fig. 1 D), which again resulted in small cellular defor-

mations (Fig. 1 E; Video S1). We note that the nature of deformation is different between adherent and suspended cells. Whereas adherent cells are locally indented by a single bead, suspended cells are squeezed between two beads, resulting in a global deformation of the cell. Nonetheless, application of pN-range forces deforms cells in the adherent and suspended state.

To take this qualitative observation to a quantifiable metric for cellular deformation in response to force, we track the position of the bead(s) over time. For measurements with adherent cells using one optical trap, the position of this single bead over time is sufficient. For measurements with suspended cells using two optical traps, we track the distance between the beads over time. As the optical trap approaches the cell, the bead initially moves through liquid and will, at some point, contact the cell. We infer this point of contact from the force curve (Fig. S1, A and B; materials and methods). The deformation of the cell at time *t* is subsequently derived by comparing the position of the bead or distance between the beads relative to the point of contact. Besides the precise spatial control over the bead position, another advantage of optical tweezers is the ability to maintain precise control over the applied force, thus ensuring uniformity across measurements. We use a force-feedback system to apply a constant load (or target force) to cells for at least 10 s. This system monitors deviations from the target force at a high frequency and adjusts the optical trap position accordingly, holding the cell in a force clamp. A typical example of a force-clamp experiment for a suspended cell is shown in Fig. 1, E–G, and Video S1. After initial bead-cell contact, the target force is reached within seconds and then stably maintained with only minor deviations (Fig. 1 F). In the corresponding force-deformation curve, two distinct stages of cellular deformation can be recognized (Fig. 1 G). First, while the force is ramping up from 0 to 100 pN, the force response is elastic (force is directly proportional to the deformation). Second, under a constant load of 100 pN, the cell exhibits viscous flow (creep) in which the deformation continues but at a slower rate (Fig. 1, F and G). This characteristic viscoelastic creep behavior is universal among different cell types and has been observed with a variety of techniques (42). Taken together, the deformation of adherent and suspended cells can be accurately quantified over time while maintaining precise control over the applied force.

Quantification of cellular mechanical properties

To further standardize our approach for quantifying cellular mechanics, we monitored cellular deformation

at two different target forces (50 and 100 pN). The standard deviation from the target force was generally less than 1.5 pN for adherent cells and $\sim 2\text{--}3$ pN for suspended cells (Fig. S2 A). The deviations are likely slightly higher for suspended cells because these cells, unlike adherent cells, are not fully immobilized. Representative force and deformation curves for suspended (Fig. 2 A) and adherent cells (Fig. 2 B) again show a rapid deformation as the force increases, with a creep response once the target force is reached. From these experiments, we can now quantify the deformation, which we define as the amount of deformation 10 s after reaching the target force. The deformations typically range from 0.2 to 1.5 μm (Fig. 2 C), depending on the applied force, with the average deformation increasing as more force is applied (Fig. 2 C). As suspended cells are, by approximation, spherical in shape, we can additionally measure the cell diameter and express the deformation as a percentage of the cell diameter (referred to as strain). The strain of suspended cells typically ranges from 5% to 15% and increases as more force is applied (Fig. S2 B). When we compare the deformation of adherent to suspended cells, we find that adherent cells deform significantly less at the same forces (Fig. 2 C).

The spring constant is a direct measure of cell stiffness, with a higher spring constant indicating that more force is required to deform the cell. We can calculate the spring constant by linearly fitting the initial elastic force response, where force is directly proportional to the deformation (Fig. 3 A). The spring constant is defined as the slope of this fit. When applying a target force of 50 pN, for suspended cells,

we find an average spring constant of 99 ± 12 pN/ μm . For adherent cells, the average spring constant is significantly higher at 267 ± 52 pN/ μm . Since we did not yet observe strain stiffening (42) when applying forces up to 100 pN, the spring constant is expected to be independent of the amount of force applied. Indeed, the average spring constant did not change when increasing the target force from 50 to 100 pN, for both suspended and adherent cells (Fig. 3 B). For both target forces, the spring constant for adherent cells is roughly twofold higher than for suspended cells (Fig. 3 B).

Next, we focused specifically on the viscous part of the force response: the deformation of cells under a constant force (referred to as creep) (Fig. 3 C, inset). We quantified the amount of creep 10 s after reaching the target force and found that cells continue to deform up to 0.4 μm in this regime (Fig. 3 D). Suspended cells generally exhibit more creep deformation than adherent cells, but this difference only reaches significance at 100 pN (Fig. 3 D). We noted that the creep response of individual cells is quite heterogeneous but, on average, can be described by an exponential decay function: $\Delta x * (1 - e^{(-t/\tau)})$, where Δx is the creep extent, t is the time, and τ is the relaxation time (Fig. S3, A and B). Here, the relaxation time τ is a measure of how quickly the creep deformation levels off under a constant force. The shape of the curves indicates that the creep response has not plateaued yet. Thus, τ offers little insight on this timescale but could be an insightful metric for longer experiments.

Together, the presented quantifications allow for direct comparison between cells experiencing different forces. In addition, we can compare the stiffness

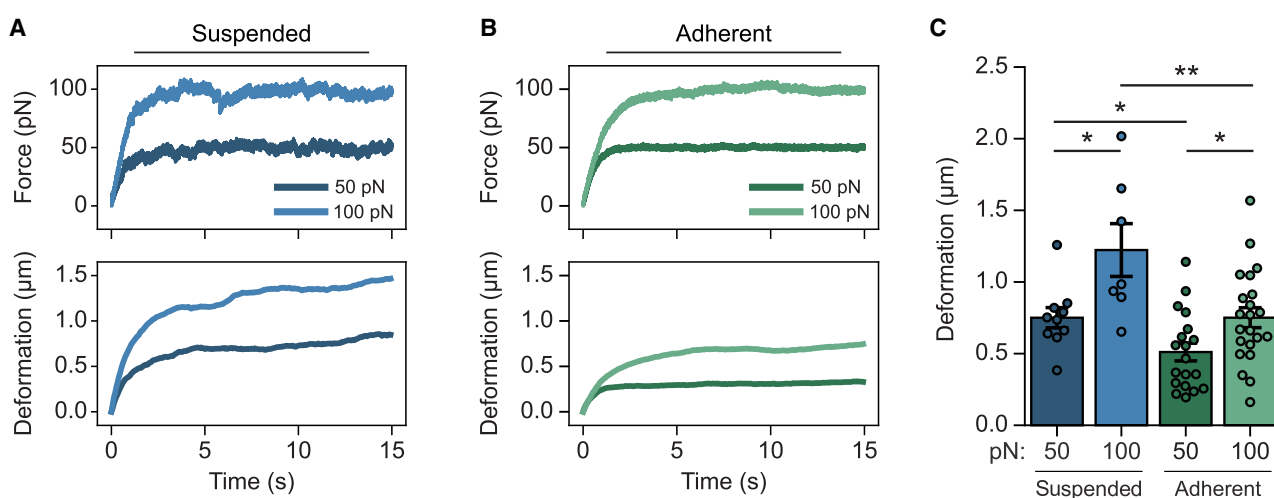


FIGURE 2 Quantification of cellular deformation. (A) Representative force (*top*) and corresponding deformation (*bottom*) curves of suspended cells deformed with a target force of 50 or 100 pN. (B) Representative force (*top*) and corresponding deformation (*bottom*) curves of adherent cells deformed with a target force of 50 or 100 pN. (C) Cellular deformation after 10 s of target force application. Data are shown as mean \pm SE. $n = 10, 7, 19,$ and 22 cells, respectively. $*p < 0.05$ and $**p < 0.01$, two-sample t -test.

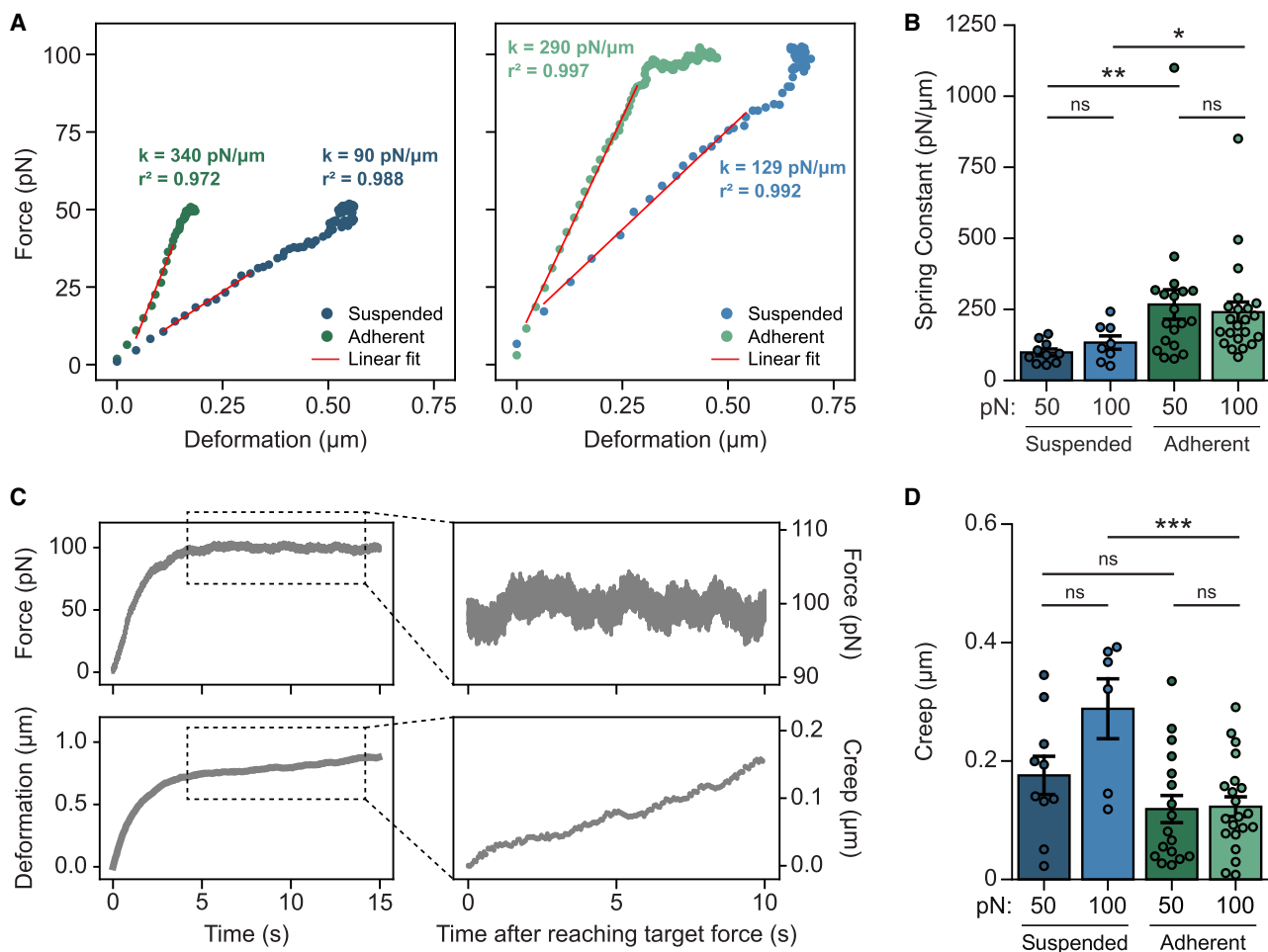


FIGURE 3 Quantifications of cellular mechanical properties. (A) Representative force-deformation curves of a suspended and an adherent cell deformed with a target force of 50 (*left*) and 100 (*right*) pN. Red lines indicate linear fits to calculate the spring constant (k). (B) Spring constants calculated from linear fits of individual curves as shown in (A). Data are shown as mean \pm SE. $n = 10, 8, 19,$ and 22 cells, respectively. $*p < 0.05$ and $**p < 0.01$, Mann-Whitney U test. (C) Representative force (*top*) and corresponding deformation (*bottom*) curves of an adherent cell deformed with a target force of 100 pN (*left*) and a zoom-in on the creep response (*right*). The creep response was monitored for 10 s after reaching the target force. (D) Creep after 10 s of target force application. Data are shown as mean \pm SE. $n = 10, 6, 17,$ and 21 cells, respectively. $***p < 0.001$, two-sample t -test.

of adherent and suspended cells. The mechanical organization of cells becomes fundamentally different when adherent cells are detached from a substrate, most notably is the absence of stress fibers in suspended cells (24). In line with these mechanical changes, we found that suspended cells are significantly more deformable at both target forces (Fig. 2 C), have a roughly twofold lower spring constant (Fig. 3 B), and exhibit more creep deformation (Fig. 3 D) compared to adherent cells—each suggesting that cells soften when detached from a substrate.

Validation using pharmacological inhibition of myosin II and actin polymerization

To validate whether our method can successfully quantify changes in cell mechanics due to mechanical

perturbations, we applied force to cells treated with inhibitors that are well known to perturb the cytoskeleton. We first treated cells seeded on a fibronectin-coated surface with 20 μM blebbistatin, an inhibitor that prevents actomyosin cross-linking by interfering with the ATPase activity of myosin II (43). Treatment with blebbistatin has previously been shown to decrease cell stiffness (44–46). Accordingly, we found that cellular deformation is significantly increased in blebbistatin-treated cells (Fig. 4, A and C). Further, the spring constant of cells almost halved in the presence of blebbistatin (Fig. 4, B and D). Thus, adherent cells significantly soften upon inhibition of myosin II activity. Interestingly, we did not find a significant difference in the creep response (Figs. 4 E and S4), suggesting that myosin II inhibition mainly affects the elastic part of the force response. Together, these

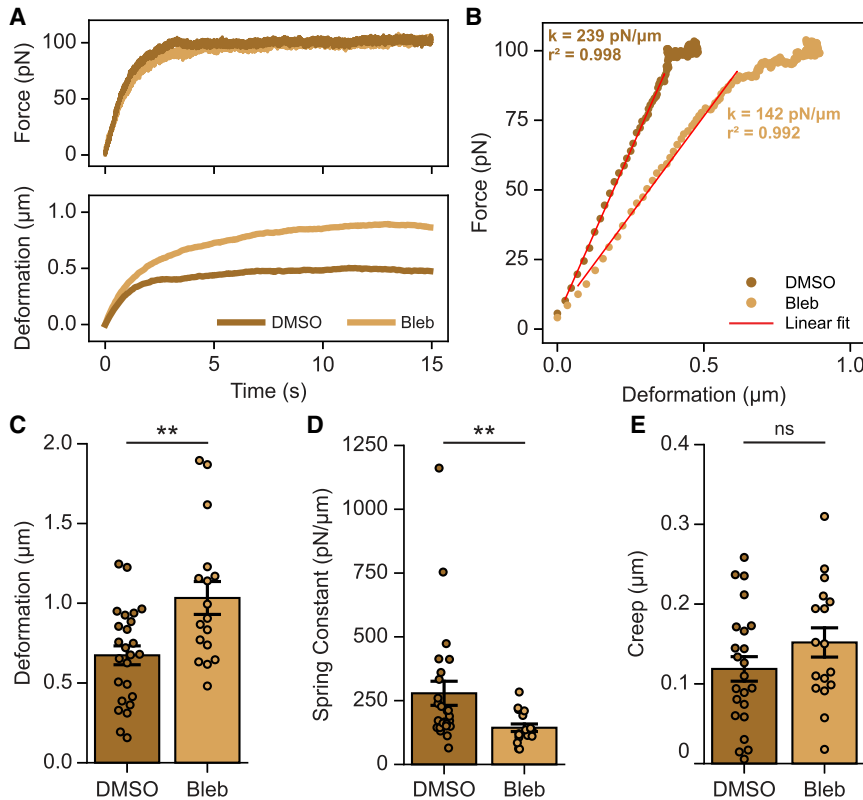


FIGURE 4 Validation using inhibition of myosin II. (A) Representative force (*top*) and corresponding deformation (*bottom*) curves of adherent cells treated with DMSO or 20 μM blebbistatin. (B) Representative force-deformation curves of adherent cells treated with DMSO or 20 μM blebbistatin. Red lines indicate linear fits used to calculate the spring constant (k). (C) Cellular deformation after 10 s of target force application. Data are shown as mean \pm SE. $n = 25$ and 17 cells, respectively. $**p < 0.01$, two-sample t -test. (D) Spring constants calculated from linear fits of individual curves as shown in (B). Data are shown as mean \pm SE. $n = 25$ and 17 cells, respectively. $**p < 0.01$, Mann-Whitney U test. (E) Creep after 10 s of target force application. Data are shown as mean \pm SE. $n = 23$ and 17 cells, respectively. $p = 0.17$, two-sample t -test.

data thus confirm that mechanical changes on adherent cells can be accurately quantified using optical tweezers.

To establish whether our approach is also able to quantify the effect of mechanical perturbations when cells are in suspension, we trypsinized and resuspended cells in medium containing 1 μM latrunculin-A, an inhibitor that prevents actin polymerization by sequestering monomeric G-actin (47). When cells are brought in the suspended state, actin forms a thick cortical layer beneath the cell membrane known as the actin cortex, which provides structural and mechanical support (24,48). Depolymerization of actin filaments using latrunculin-A is, therefore, expected to soften cells. Indeed, we found that suspended cells treated with latrunculin-A are highly deformable, with the average deformation and strain increasing approximately fourfold compared to untreated cells (Figs. 5, A and C and S5, A and B). Similarly, the spring constant of suspended cells is greatly reduced in the presence of latrunculin-A (Fig. 5, B and D). Finally, latrunculin-A-treated cells exhibited significantly more creep deformation (Figs. 5 E and S5 C). These results confirm that the actin cortex of suspended cells is key to providing resistance to external force. Collectively, these data show that optical tweezers can accurately detect changes in mechanical properties upon perturbation when cells are in the suspended state.

DISCUSSION

Here, we demonstrated the use of optical tweezers for mechanical measurements on adherent and suspended cells. Our approach allows for the quantification of cellular deformation, the spring constant, and the creep response from a single force-deformation curve. By keeping the optical trap position under the control of a force-feedback system, we show that forces can be precisely applied to cells with minimal deviations, thus ensuring uniformity across measurements. Using drug-induced perturbations of the cytoskeleton, we show that this approach is sensitive to detecting changes in the mechanical properties of both adherent and suspended cells.

Studies using optical tweezers to quantify cellular mechanics are limited and mostly measured on red blood cells, in part due to their mechanical and structural simplicity, allowing for large cellular deformations even under relatively small forces. In these studies, two optically trapped beads are adhered to the surface of a red blood cell. Subsequently, one bead is displaced to stretch the cell while its deformation is recorded (36–41). A similar approach has recently been used for mechanical characterization of suspended fibroblasts (49) and monocytes (50). In this experimental setup, variability in bead-cell attachment may reduce experimental robustness. We and

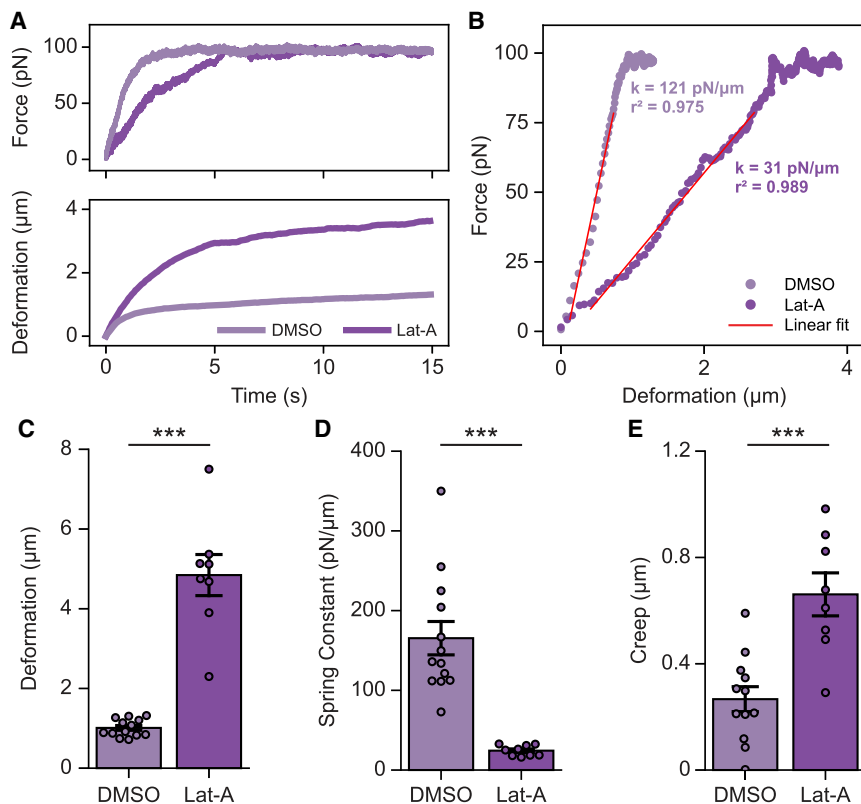


FIGURE 5 Validation using inhibition of actin polymerization. (A) Representative force (top) and corresponding deformation (bottom) curves of suspended cells treated with DMSO or 1 μM latrunculin-A. (B) Representative force-deformation curves of suspended cells treated with DMSO or 1 μM latrunculin-A. Red lines indicate linear fits used to calculate the spring constant (k). (C) Cellular deformation after 10 s of target force application. Data are shown as mean \pm SE. $n = 13$ and 8 cells, respectively. *** $p < 0.001$, two-sample t -test. (D) Spring constants calculated from linear fits of individual curves as shown in (B). Data are shown as mean \pm SE. $n = 13$ and 9 cells, respectively. *** $p < 0.001$, two-sample t -test. (E) Creep after 10 s of target force application. Data are shown as mean \pm SE. $n = 12$ and 8 cells, respectively. *** $p < 0.001$, two-sample t -test.

others focused on the indentation rather than the stretching of cells. For example, the indentation of adherent cells using optical tweezers was accomplished along the axial direction using a single optically trapped bead (19,51,52), with forces reaching up to ~ 20 pN. We indent cells along the lateral rather than the axial direction, which has the advantage that it is applicable to both adherent and suspended cells. Furthermore, in contrast to previous work, we kept the optical trap under the control of a force-feedback system to precisely apply the same amount of force to each cell. The use of a force-feedback system additionally allows us to quantify the creep response of cells, i.e., how the deformation evolves over time under a constant amount of force.

In addition to single-cell methods (such as AFM and optical/magnetic tweezers), several high-throughput techniques have been developed in recent years. For example, flow systems are used to deform suspended cells by lasers (optical stretching (53)) or shear fluid forces (22,23). Another recently developed technique is acoustic force spectroscopy, in which several cells are stretched simultaneously by pulling beads that are attached to cells toward an acoustic node (54). An important advantage of these techniques is the rapid screening of many cells in a short time compared to optical tweezers or other single-cell methods (only several cells per hour). These high-throughput

techniques are particularly powerful for a rapid comparison of two (or more) populations of cells, whereas single-cell methods provide higher sensitivity and a more extensive description of mechanical properties on a single-cell level.

Although optical tweezers enable accurate force application and quantification at pN resolution, it does come at the expense of a relatively low force limit, which is typically 200–400 pN. Other contact-based methods, including AFM and magnetic tweezers, can reach higher (nN-range) forces, but such forces can induce damage to the cell (20), and may even deform the underlying substrate (44). Our results using blebbistatin and latrunculin-A show that pN-range forces are sufficient to accurately measure the effect of these perturbations on cellular mechanics. Thus, measurements under controlled but relatively small forces, which are often unattainable with other techniques, are well suited to accurately measure changes in mechanical properties. Importantly, stiffness measurements can be influenced by the shape of the probe used to apply force (55). It is therefore critical that comparisons of the mechanical properties measured with any contact-based method are done using probes of the same geometry.

Our current understanding of cell mechanics has mostly been gained from mechanical measurements on adherent cells. We show that optical tweezers

can accurately measure on adherent cells as well as on suspended cells, which has several advantages. First, the actin cytoskeleton is heterogeneously organized in adherent cells, with stress fibers spanning from one focal adhesion point to another. The measured stiffness of cells can therefore be profoundly different when probed in an area with high or low abundance of stress fibers (56). Suspended cells have a more homogeneously organized cytoskeleton, so the quantification of mechanical properties is less dependent on the location of force application. Second, surface modification can directly affect the quantification of cell stiffness (4,5,8), which is ruled out when cells are in the suspended state. Finally, this approach is attractive for mechanical characterization of naturally nonadherent cells such as immune cells, which strongly rely on their mechanical organization for normal functioning (57).

In conclusion, our findings show that optical tweezers are suitable for the robust quantification of cell mechanics. We provide a straightforward method to extract several mechanical properties from a single experiment. The combination with confocal microscopy provides interesting opportunities for the visualization of the cellular mechanical response to calibrated forces.

ACKNOWLEDGMENTS

We thank the Radboud UMC Technology Center Microscopy for use of their microscopy facilities and Marieke Willemse and Koen van den Dries for generously sharing reagents.

AUTHOR CONTRIBUTIONS

W.S.R. and J.M.E. conceived the project. W.S.R. and S.F.A.E. performed experiments. W.S.R. analyzed data. W.S.R. and J.M.E. wrote the manuscript with input from all authors.

DECLARATION OF INTERESTS

The authors declare no competing interests.

SUPPORTING MATERIAL

Supplemental information can be found online at <https://doi.org/10.1016/j.bpr.2025.100199>.

REFERENCES

- Martino, F., A. R. Perestrelo, ..., G. Forte. 2018. Cellular Mechano-transduction: From Tension to Function. *Front. Physiol.* 9:824.
- Discher, D. E., P. Janmey, and Y. L. Wang. 2005. Tissue Cells Feel and Respond to the Stiffness of Their Substrate. *Science*. 310:1139–1143.
- Mathur, A. B., A. M. Collinsworth, ..., G. A. Truskey. 2001. Endothelial, cardiac muscle and skeletal muscle exhibit different viscous and elastic properties as determined by atomic force microscopy. *J. Biomech.* 34:1545–1553.
- Solon, J., I. Levental, ..., P. A. Janmey. 2007. Fibroblast Adaptation and Stiffness Matching to Soft Elastic Substrates. *Biophys. J.* 93:4453–4461.
- Janmey, P. A., D. A. Fletcher, and C. A. Reinhart-King. 2020. Stiffness Sensing by Cells. *Physiol. Rev.* 100:695–724.
- Lautenschläger, F., S. Paschke, ..., J. Guck. 2009. The regulatory role of cell mechanics for migration of differentiating myeloid cells. *Proc. Natl. Acad. Sci. USA.* 106:15696–15701.
- Dupont, S., and S. A. Wickström. 2022. Mechanical regulation of chromatin and transcription. *Nat. Rev. Genet.* 23:624–643.
- Engler, A. J., S. Sen, ..., D. E. Discher. 2006. Matrix Elasticity Directs Stem Cell Lineage Specification. *Cell.* 126:677–689.
- Vining, K. H., and D. J. Mooney. 2017. Mechanical forces direct stem cell behaviour in development and regeneration. *Nat. Rev. Mol. Cell Biol.* 18:728–742.
- Shiraishi, K., P. P. Shah, ..., E. E. Morrissey. 2023. Biophysical forces mediated by respiration maintain lung alveolar epithelial cell fate. *Cell.* 186:1478–1492.e15.
- Sun, Y., L. G. Villa-Diaz, ..., J. Fu. 2012. Mechanics Regulates Fate Decisions of Human Embryonic Stem Cells. *PLoS One.* 7:e37178.
- Phillip, J. M., I. Aifuwa, ..., D. Wirtz. 2015. The Mechanobiology of Aging. *Annu. Rev. Biomed. Eng.* 17:113–141.
- Bajpai, A., R. Li, and W. Chen. 2021. The cellular mechanobiology of aging: from biology to mechanics. *Ann. N. Y. Acad. Sci.* 1491:3–24.
- Wirtz, D., K. Konstantopoulos, and P. C. Searson. 2011. The physics of cancer: the role of physical interactions and mechanical forces in metastasis. *Nat. Rev. Cancer.* 11:512–522.
- Gensbittel, V., M. Kräter, ..., J. G. Goetz. 2021. Mechanical Adaptability of Tumor Cells in Metastasis. *Dev. Cell.* 56:164–179.
- Zuela-Sopilniak, N., and J. Lammerding. 2022. Can't handle the stress? Mechanobiology and disease. *Trends Mol. Med.* 28:710–725.
- Hobson, C. M., M. R. Falvo, and R. Superfine. 2021. A survey of physical methods for studying nuclear mechanics and mechanobiology. *APL Bioeng.* 5:041508.
- Bull, M. S., R. M. A. Sullan, ..., T. T. Perkins. 2014. Improved single molecule force spectroscopy using micromachined cantilevers. *ACS Nano.* 8:4984–4995.
- Nawaz, S., P. Sánchez, ..., I. A. T. Schaap. 2012. Cell Visco-Elasticity Measured with AFM and Optical Trapping at Sub-Micrometer Deformations. *PLoS One.* 7:e45297.
- Haase, K., and A. E. Pelling. 2015. Investigating cell mechanics with atomic force microscopy. *J. R. Soc. Interface.* 12:20140970.
- Hochmuth, R. M. 2000. Micropipette aspiration of living cells. *J. Biomech.* 33:15–22.
- Urbanska, M., H. E. Muñoz, ..., J. Guck. 2020. A comparison of microfluidic methods for high-throughput cell deformability measurements. *Nat. Methods.* 17:587–593.
- Otto, O., P. Rosendahl, ..., J. Guck. 2015. Real-time deformability cytometry: on-the-fly cell mechanical phenotyping. *Nat. Methods.* 12:199–202.
- Chan, C. J., A. E. Ekpenyong, ..., F. Lautenschläger. 2015. Myosin II Activity Softens Cells in Suspension. *Biophys. J.* 108:1856–1869.
- Bustamante, C. J., Y. R. Chemla, ..., M. D. Wang. 2021. Optical tweezers in single-molecule biophysics. *Nat. Rev. Methods Primers.* 1:25.
- Zhang, H., and K.-K. Liu. 2008. Optical tweezers for single cells. *J. R. Soc. Interface.* 5:671–690.
- Català-Castro, F., E. Schäffer, and M. Krieg. 2022. Exploring cell and tissue mechanics with optical tweezers. *J. Cell Sci.* 135:jcs259355.

28. Titushkin, I., and M. Cho. 2006. Distinct membrane mechanical properties of human mesenchymal stem cells determined using laser optical tweezers. *Biophys. J.* 90:2582–2591.
29. Campillo, C., P. Sens, ..., C. Sykes. 2013. Unexpected membrane dynamics unveiled by membrane nanotube extrusion. *Biophys. J.* 104:1248–1256.
30. Hurst, S., B. E. Vos, ..., T. Betz. 2021. Intracellular softening and increased viscoelastic fluidity during division. *Nat. Phys.* 17:1270–1276.
31. Schreiner, S. M., P. K. Koo, ..., M. C. King. 2015. The tethering of chromatin to the nuclear envelope supports nuclear mechanics. *Nat. Commun.* 6:7159.
32. Bergamaschi, G., A. S. Biebricher, ..., G. J. L. Wuite. 2024. Heterogeneous force response of chromatin in isolated nuclei. *Cell Rep.* 43:114852.
33. Falleroni, F., V. Torre, and D. Cojoc. 2018. Cell Mechanotransduction With Piconewton Forces Applied by Optical Tweezers. *Front. Cell. Neurosci.* 12:130.
34. Sergides, M., L. Perego, ..., M. Capitanio. 2021. Probing mechanotransduction in living cells by optical tweezers and FRET-based molecular force microscopy. *Eur. Phys. J. A.* 136:316.
35. Vasse, G. F., P. Buzón, ..., P. van Rijn. 2021. Single Cell Reactomics: Real-Time Single-Cell Activation Kinetics of Optically Trapped Macrophages. *Small Methods.* 5:e2000849.
36. Sleep, J., D. Wilson, ..., W. Gratzler. 1999. Elasticity of the red cell membrane and its relation to hemolytic disorders: an optical tweezers study. *Biophys. J.* 77:3085–3095.
37. Dao, M., C. T. Lim, and S. Suresh. 2003. Mechanics of the human red blood cell deformed by optical tweezers. *J. Mech. Phys. Solid.* 51:2259–2280.
38. Lim, C. T., M. Dao, ..., K. T. Chew. 2004. Large deformation of living cells using laser traps. *Acta Mater.* 52:1837–1845.
39. Mills, J. P., M. Diez-Silva, ..., S. Suresh. 2007. Effect of plasmodial RESA protein on deformability of human red blood cells harboring *Plasmodium falciparum*. *Proc. Natl. Acad. Sci. USA.* 104:9213–9217.
40. Betz, T., M. Lenz, ..., C. Sykes. 2009. ATP-dependent mechanics of red blood cells. *Proc. Natl. Acad. Sci. USA.* 106:15320–15325.
41. Gironella-Torrent, M., G. Bergamaschi, ..., F. Ritort. 2024. Viscoelastic phenotyping of red blood cells. *Biophys. J.* 123:770–781. <https://doi.org/10.1016/j.bpj.2024.01.019>.
42. Moeendarbary, E., and A. R. Harris. 2014. Cell mechanics: principles, practices, and prospects. *WIREs Mechanisms of Disease.* 6:371–388.
43. Kovács, M., J. Tóth, ..., J. R. Sellers. 2004. Mechanism of Blebbistatin Inhibition of Myosin II. *J. Biol. Chem.* 279:35557–35563.
44. Rheinlaender, J., A. Dimitracopoulos, ..., K. Franze. 2020. Cortical cell stiffness is independent of substrate mechanics. *Nat. Mater.* 19:1019–1025.
45. Moeendarbary, E., L. Valon, ..., G. T. Charras. 2013. The cytoplasm of living cells behaves as a poroelastic material. *Nat. Mater.* 12:253–261.
46. Martens, J. C., and M. Radmacher. 2008. Softening of the actin cytoskeleton by inhibition of myosin II. *Pflügers Archiv.* 456:95–100.
47. Coué, M., S. L. Brenner, ..., E. D. Korn. 1987. Inhibition of actin polymerization by latrunculin A. *FEBS Lett.* 213:316–318.
48. Flormann, D. A. D., L. Kainka, ..., F. Lautenschläger. 2024. The structure and mechanics of the cell cortex depend on the location and adhesion state. *Proc. Natl. Acad. Sci. USA.* 121:e2320372121.
49. Schlosser, F., F. Rehfeldt, and C. F. Schmidt. 2015. Force fluctuations in three-dimensional suspended fibroblasts. *Phil. Trans. R. Soc. B.* 370:20140028.
50. Evers, T. M. J., V. Sheikhsani, ..., A. Mashaghi. 2022. Single-cell analysis reveals chemokine-mediated differential regulation of monocyte mechanics. *iScience.* 25:103555.
51. Coceano, G., M. S. Yousafzai, ..., E. Ferrari. 2016. Investigation into local cell mechanics by atomic force microscopy mapping and optical tweezer vertical indentation. *Nanotechnology.* 27:065102.
52. Yousafzai, M. S., F. Ndoye, ..., D. Cojoc. 2016. Substrate-dependent cell elasticity measured by optical tweezers indentation. *Opt Laser. Eng.* 76:27–33.
53. Guck, J., R. Ananthakrishnan, ..., J. Käs. 2001. The Optical Stretcher: A Novel Laser Tool to Micromanipulate Cells. *Biophys. J.* 81:767–784.
54. Sorkin, R., G. Bergamaschi, ..., G. J. L. Wuite. 2018. Probing cellular mechanics with acoustic force spectroscopy. *MBoC.* 29:2005–2011.
55. Kulkarni, S. G., S. Pérez-Domínguez, and M. Radmacher. 2023. Influence of cantilever tip geometry and contact model on AFM elasticity measurement of cells. *JMR (J. Mol. Recognit.).* 36:e3018.
56. Maloney, J. M., D. Nikova, ..., K. J. Van Vliet. 2010. Mesenchymal Stem Cell Mechanics from the Attached to the Suspended State. *Biophys. J.* 99:2479–2487.
57. Huse, M. 2017. Mechanical forces in the immune system. *Nat. Rev. Immunol.* 17:679–690.